

原位反应合成四唑金属配位聚合物:结构与磁性

李如茵 高 松*

(北京分子科学国家实验室, 稀土材料化学及应用国家重点实验室,
北京大学化学与分子工程学院, 北京 100871)

摘要: 使用 Demko-Sharpless 方法, 在溶剂热条件下可以安全、有效地获得含四唑基团的配体。基于此反应, 引入叠氮短桥共配, 获得了 2 个结构新颖的配位聚合物 $\text{Co}_3(3\text{-ptz})_4(\text{N}_3)_2(\text{H}_2\text{O})_2 \cdot 4\text{H}_2\text{O}$ (**1**) 与 $\text{Mn}_3(3\text{-ptz})_2(\text{N}_3)_4(\text{H}_2\text{O}) \cdot 0.5\text{H}_2\text{O}$ (**2**)。2 个配合物中, 通过反应获得的桥连配体 3-(pyridinyl)tetrazole(3-ptz)阴离子与过量的叠氮作为短桥参与, 均采取了多种配位模式, 使得化合物具有复杂的结构。同时, 四唑阴离子和叠氮均传递磁耦合作用。

关键词: 四唑; 叠氮; 钴; 锰; 结构; 磁性

中图分类号: O614.7⁺11; O614.81⁺2

文献标识码: A

文章编号: 1001-4861(2008)08-1229-08

Two Magnetic Metal Coordination Polymers with Tetrazolyl Ligands through *in situ* Reactions

LI Ru-Yin GAO Song*

(Beijing National Laboratory for Molecular Sciences, State Key Lab of Rare Earth Materials Chemistry and Applications,
College of Chemistry and Molecular Engineering, Peking University, Beijing 100871)

Abstract: The Demko-Sharpless' is a very effective method for synthesis of the tetrazole compounds. Using this method, two coordination polymers have been obtained using solvent thermal reactions, and characterized structurally and magnetically. The 2D layer **1**, $\text{Co}_3(3\text{-ptz})_4(\text{N}_3)_2(\text{H}_2\text{O})_2 \cdot 4\text{H}_2\text{O}$ is consisted of 1D azido-bridged Co^{2+} chains linked through the coordinated Co^{2+} building block. The 3D network **2**, $\text{Mn}_3(3\text{-ptz})_2(\text{N}_3)_4(\text{H}_2\text{O}) \cdot 0.5\text{H}_2\text{O}$ is consisted with complicated 2D azido-bridged Mn^{2+} layers pillared by bridge ligands. The excessive azide ions in the reaction adopt μ -1,1, μ -1,3 modes in **1** and μ -1,1, μ -1,3, μ -1,1,3 modes in **2**, bridge the neighboring metal ions and transmit magnetic couplings. The 3-(pyridinyl)tetrazole anion, which is the production of the Demko-Sharpless' reaction, bridges with bidentate and tridentate mode in **1**, with tridentate and pentadentate mode in **2**. They not only bridge the metal ions, but also transmit magnetic couplings along with azide ions. CCDC: 687278, **1**; 687279, **2**.

Key words: tetrazole; azide; cobalt; manganese; structure; magnetism

Tetrazole function groups are widely used in coordination chemistry because of their wonderful coordination ability and various bridging modes. Plenty of coordination polymers with intriguing crystal structures and interesting physical properties have been

synthesized using tetrazole derivations. The application value of them in materials with ferroelectricity, fluorescent properties, optical properties, SHG properties and high energy densities makes it still an attractive research field^[1-4]. But the main deficient in

收稿日期: 2008-05-13. 收修改稿日期: 2008-06-26.

国家自然科学基金(No.20221101, 20490210)、科技部 973(No.2006CB601102)资助项目。

*通讯联系人。E-mail: gaosong@pku.edu.cn; Tel: 010-62767569

第一作者: 李如茵, 女, 25 岁, 博士研究生; 研究方向: 配位化学与分子磁性。

synthesis is the complicated and toxic approaches. A brand new period is start from the Demko-Sharpless' reaction that was reported in 2001^[5-9]. This in situ reaction becomes the safest and mildest method to obtain high quality crystals of coordination polymers containing 5-substituted 1H-tetrazole ligand in ordinary hydrothermal conditions^[10,11]. The most remarkable characteristic of Demko-Sharpless' reaction is that it provides possibility to obtain extremely novel compounds in the [3 +2] formation process, that are rarely obtained in normal experiments. Take tetrazole anion for instance, it could offer all four nitrogen atoms to coordinate. When combined with other substitute function groups such as pyridine rings, the tetrazole derivation compound becomes a powerful bridge ligand.

Much attention has been focus on the synthesis and investigation of metal-organic frameworks obtained by this method with certain transition metal centers, such as Zn^{2+} , Cd^{2+} , Cu^2 , Mn^2 , Ag^+ and so on^[12-19]. The fabulous coordination ability of them along with multi coordination modes of tetrazole derivations result a lot of novel crystal structures. Most of these compounds consist of an extended 2D or 3D structure^[20]. However, only a few paramagnetic transition metal ions have been investigated in such method to obtain magnetic coordination polymers^[21]. It's attractive for us to seek the magnetic properties of a compound with such complicated structure. In this context, we design two

compounds and obtain by Demko-Sharpless' reaction, $\text{Co}_3(3\text{-ptz})_4(\text{N}_3)_2(\text{H}_2\text{O})_2 \cdot 4\text{H}_2\text{O}$ (**1**) and $\text{Mn}_3(3\text{-ptz})_2(\text{N}_3)_4(\text{H}_2\text{O}) \cdot 0.5\text{H}_2\text{O}$ (**2**) (3-ptz=3-(pyridinyl)tetrazole), with 2D and 3D structures, respectively. The 3-(pyridinyl) tetrazole anions act as bidentate and tridentate bridges in **1**, and pentadentate and tridentate bridge in **2**. A rational design is to use excessive ratio of azide ions which act as short bridge adopt μ -1,1, μ -1,3, and μ -1,1,3 modes to bridge, transmit magnetic couplings effectively between metal ions.

1 Experimental procedures

1.1 Materials and apparatus

All starting materials were commercially available, reagents of analytical grade and were used without further purification. Elemental analyses were carried out using an Elementary Vario EL analyzer.

Crystallographic data of **1** and **2** were collected at 293 K on a Nonius κ -CCD diffractometer. Empirical absorption corrections were applied using Sortav program. The structure was solved by the direct method and refined using the SHELX-97 program. Full-matrix least-squares method on F^2 with anisotropy thermal parameters had been used for all non-hydrogen atoms. Hydrogen atoms are placed by the calculated positions, and refined isotropically^[22-27]. Crystallographic data and structure refinement results are summarized in Table 1.

CCDC: 687278, **1**; 687279, **2**.

Table 1 Crystallographic data and structure refinement results for **1**·Co and **2**·Mn

Compound	1 ·Co	2 ·Mn
Formula	$\text{C}_{24}\text{H}_{36}\text{Co}_3\text{N}_{26}\text{O}_6$	$\text{C}_{12}\text{H}_{11}\text{Mn}_3\text{N}_{22}\text{O}_{1.5}$
Formula weight	961.52	652.19
Crystal system	Monoclinic	Orthorhombic
Space group	$P2_1/n$	$Pbca$
<i>Z</i>	2	8
<i>a</i> / nm	0.866 11(2)	1.523 12(3)
<i>b</i> / nm	0.811 58(2)	1.347 93(3)
<i>c</i> / nm	2.689 80(9)	2.623 54(6)
β / (°)	96.7060(8)	
<i>V</i> / nm ³	1.877 7(7)	5.385 1(1)
<i>D_c</i> / (g·cm ⁻³)	1.669	1.591
μ / mm ⁻¹	1.387	1.439
Reflections collected / Unique (<i>R_{int}</i>)	17 738 / 3 276 (0.125 2)	8 954 / 4 730 (0.074 1)
Data / restraints / parameters	3 276 / 0 / 267	4 730 / 0 / 349

Table 1

Final R indices [$I > 2\sigma(I)$]	$R_1=0.078\ 5$, $wR_2=0.207\ 3$	$R_1=0.048\ 9$, $wR_2=0.118\ 5$
R indices (all data)	$R_1=0.141\ 5$, $wR_2=0.246\ 3$	$R_1=0.119\ 3$, $wR_2=0.135\ 6$
GOF	1.013	0.909

$$^{[a]} R_1 = \sum ||F_o| - |F_c|| / \sum F_o; \quad ^{[b]} wR_2 = \{ \sum [w(F_o^2 - F_c^2)^2] / \sum [w(F_o^2)] \}^{1/2}.$$

Magnetic data of the compounds were obtained on a Quantum Design MPMS-XL5 SQUID system. The experimental susceptibility was corrected for diamagnetism (Pascal's tables)^[28].

1.2 Preparation of $\text{Co}_3(\text{3-ptz})_4(\text{N}_3)_2(\text{H}_2\text{O})_2 \cdot 4\text{H}_2\text{O}$ (1)

A methanol solution (3 mL) of $\text{Co}(\text{NO}_3)_2$ (0.5 mmol) and NaN_3 (2.0 mmol) was mixed with a methanol solution (6 mL) of 3-cyanopyridine (0.5 mmol). After heating at 130 °C for 3 days, the mixture was cooling to the room temperature slowly. Red crystals with needle shape of **1** were obtained and separated manually (yield 10%). IR/ cm^{-1} : 3 320b,m, 2 930b,w, 2 140s, 2 120s, 2 070s, 1 620w, 1 590w, 1 430w, 1 370w, 1 360w, 1 270w, 1 200w, 1 060w, 1 020w, 814w, 769w, 758w, 739w, 710w, 700w, 677w cm^{-1} . Elemental anal. Calcd for $\text{C}_{24}\text{H}_{36}\text{N}_{26}\text{O}_6\text{Co}_3$ (%): C, 29.97; N, 37.87; H, 3.77. Found (%): C, 30.36; N, 37.08; H, 3.39.

1.3 Preparation of $\text{Mn}_3(\text{3-ptz})_2(\text{N}_3)_4(\text{H}_2\text{O}) \cdot 0.5\text{H}_2\text{O}$ (2)

An aqueous solution (4 mL) of MnCl_2 (0.5 mmol) and NaN_3 (2.0 mmol) was mixed with a methanol solution (2 mL) of 3-cyanopyridine (0.5 mmol). With the same experimental procedures with **1**, needle shaped, yellow crystals of **2** were obtained (yield 60%). IR/ cm^{-1} : 3 450m, 3 380m, 3 330m, 2 120s, 2 070s, 1 620w, 1 460 w, 1 430m, 1 370w, 1 330w, 1 280w, 1 130w, 1 030w, 818 w, 756w, 706w, 660w. Calcd for $\text{C}_{12}\text{H}_{11}\text{N}_{22}\text{O}_{1.5}\text{Mn}_3$ (%): C, 22.09; N, 47.25; H, 1.68. Found (%): C, 21.92; N, 47.74; H, 2.08.

CAUTION: Although not encountered in our experiment, azido salts and complexes of metal ions are potentially explosive. Only a small amount of materials should be prepared, and handled with care.

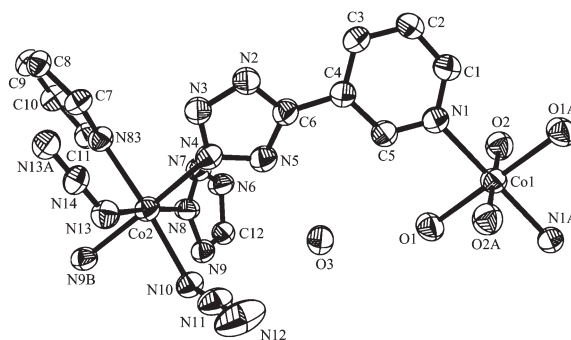
2 Results and discussions

In this reaction, tetrazole rings of 3-(pyridinyl) tetrazole anions are formed. It act bridge ligands with

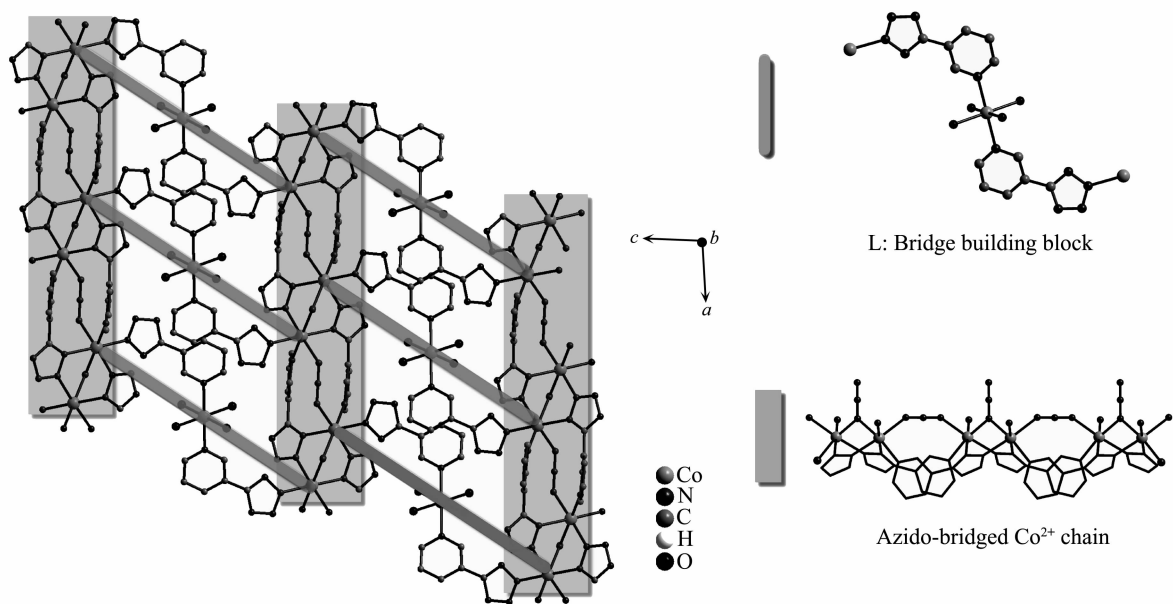
bidentate, tridentate and pentadentate modes while coordinate. In order to introduce azide ions to coordinate as the co-ligand and transmit magnetic couplings, excessive reagent sodium azide are added four times to the metal ions. This strategy has been used before^[29]. Both the tetrazole rings and the azide ions have various coordination modes. The combination of azide ions and 3-(pyridinyl)tetrazole results in two coordination polymers with extremely complicated net structures.

2.1 Crystal structure

Compound **1** crystallizes in the monoclinic space group $P2_1/n$. The symmetrical unit consists of two octahedrally coordinated Co^{2+} ions, as shown in Fig.1 and Fig.2. The geometries of them are listed in Table 2. The crystal structure of **1** can be divided into two individual parts: the azido-bridged $\text{Co}(1)^{2+}$ 1D chain and the coordinated $\text{Co}(2)^{2+}$ bridge building block L. Both of them contain 3-(pyridinyl)tetrazole anions as bridge ligands, which acts as tridentate bridge ligand in the azido-bridged $\text{Co}(1)^{2+}$ chain, and acts as bidentate bridge ligand in the coordinated bridge building block L. The connection between these two parts constructs a 2D layer.

Fig.1 Coordination environment of **1**

The azido-bridged $\text{Co}(1)^{2+}$ 1D chain is constructed by EE and EO mode azide ions, tridentate 3-(pyridinyl) tetrazole and $\text{Co}(1)^{2+}$ ions. Each Co^{2+} ion has a distorted octahedral symmetry. The equatorial positions of the

Fig.2 Two parts of the 2D layer of **1****Table 2** Selected bond lengths (nm) and angles (°) for **1**·Co

Co(1)-O(2) ^a	0.207 2(6)	Co(2)-N(4)	0.211 3(6)	Co(1)-N(1) ^a	0.214 2(6)
Co(1)-O(2)	0.207 2(6)	Co(2)-N(10)	0.212 7(5)	Co(2)-N(8)	0.214 5(6)
Co(1)-O(1) ^a	0.212 9(6)	N(10)-Co(2) ^b	0.212 7(5)	Co(2)-N(13)	0.223 9(6)
Co(1)-O(1)	0.212 9(6)	N(9)-Co(2) ^b	0.218 2(7)	Co(2)-N(83)	0.217 6(6)
Co(1)-N(1)	0.214 2(6)	Co(2)-N(9) ^b	0.218 2(7)		
N(3)-N(4)-Co(2)	122.9(5)	N(83)-Co(2)-N(9) ^b	87.8(2)	N(10)-Co(2)-N(9) ^b	84.6(2)
O(2)a-Co(1)-O(2)	180.0(3)	N(9)b-Co(2)-N(13)	91.6(2)	N(8)-Co(2)-N(9) ^b	89.0(2)
O(2)a-Co(1)-O(1) ^a	88.2(2)	N(14)-N(13)-Co(2)	131.2(5)	C(12)-N(9)-Co(2) ^b	140.5(5)
O(2)-Co(1)-O(1) ^a	91.8(2)	N(11)-N(10)-Co(2)	124.9(2)	N(8)-N(9)-Co(2) ^b	114.4(4)

^a -x+1, -y+1, -z+1; ^b -x+1/2, y, -z+3/2; ^c -x-1/2, y, -z+3/2.

Co²⁺ ion are occupied by four nitrogen atoms from three tetrazole rings and one azide ion, and the axial positions of the Co²⁺ ion are coordinated with two nitrogen atoms from azide ion and 3-pyridinyl ring. The neighboring Co(1)²⁺ ions are connected through EO azide ions and dual bidentate tetrazole rings into dimers as shown in Fig.1, with the distance Co1A...Co1B=0.348 7 nm. The neighboring dimers are linked through one EE azide ion and two bidentate 3-(pyridinyl)tetrazole anions as bridge ligands, and are extended into 1D chain along *a* axis as shown in Fig.2. The nearest distance between neighboring dimers is Co1B...Co1C=0.574 0 nm, the Co-N_{azide}-N_{azide} angles are of 131.24°, the torsion angle of the EE azide ion is of 79.60°. Thus, the azido-bridged Co²⁺ 1D chains own alternate arrangement of EE/EO

azido linkages, along with the corresponding tetrazole/3-(pyridinyl)tetrazole alternate arrangement. This kind of 1D structure has been observed in a Cd²⁺ complex before^[30]. However, in Cd²⁺ complex, the 1D chain is twisted into a channel. Been occupied by azide ions and a 3-(pyridinyl)tetrazole ligand with five coordination positions, the remaining one coordination position is linked to the second crystallographically independent Co²⁺ ion through another part of 3-(pyridinyl)tetrazole ligands, which will be described later.

The second crystallographically independent Co²⁺ ion locates between neighboring chains. It is equatorially coordinated with four oxygen atoms from water molecules and axially coordinated with two pyridine nitrogen atoms of the bridge ligand 3-

(pyridinyl)tetrazole. The coordination of $\text{Co}(2)^{2+}$ and two 3-(pyridinyl)tetrazole ligands makes them become a brand new bridge ligand as a coordinated building block L that connects neighboring azido-bridged $\text{Co}(1)^{2+}$ chains into a 2D layer. In contrast to the tridentate 3-(pyridinyl)tetrazole ligands in azido-bridged chain, the 3-(pyridinyl)tetrazole ligand in this L only acts as bidentate ligand, and it uses only one tetrazole nitrogen atom to coordinate with $\text{Co}(1)$ and one pyridine nitrogen atom to coordinate with $\text{Co}(2)$. The distance between $\text{Co}(1)$ and $\text{Co}(2)$ is 0.855 3 nm. The nearest distance between neighboring chains is $\text{Co1A} \cdots \text{Co1D}=1.453\ 2$ nm. The distance between Co^{2+} ions which are linked through the coordinated building block is $\text{Co1A} \cdots \text{Co1E}=1.710\ 6$ nm, while it is only the third nearest distance between the Co^{2+} ions on neighboring chains. This is mainly because its coordination points are on the slightly inboard side as shown in Fig.2, which enables L a distorted coordinate configuration. Besides, the rigid fragment and large volume results a large steric hindrance, which makes it lies inclined to the chains and connects the metal ions only with suitable distances.

The connection of L among chains results in a fluctuant 2D layer as the cross section shown in Fig.3. H-bond has been discovered inside the 2D layer, with the geometry of $\text{O} \cdots \text{N}=0.268\ 5$ nm, $\text{O}-\text{H} \cdots \text{N}=133.22^\circ$. As shown in Fig.3, the neighboring 2D layers are

stacked by H-bond with the distance $\text{O} \cdots \text{N}=0.267\ 9$ nm, the angle $\text{O}-\text{H} \cdots \text{N}=99.83^\circ$. The nearest distance of Co^{2+} ions among neighboring layers is $\text{Co1} \cdots \text{Co1}=0.811\ 6$ nm, and the value of $\text{Co2} \cdots \text{Co2}$ is 0.811 6 nm.

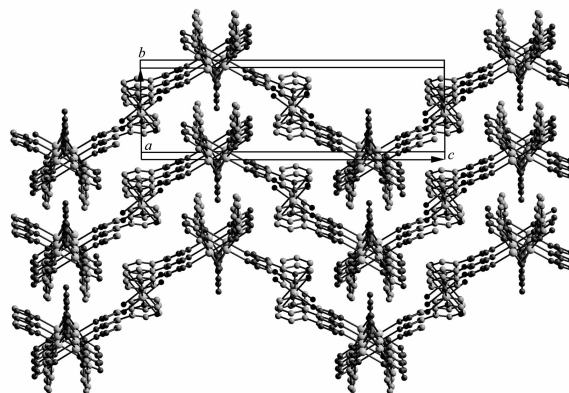


Fig.3 Packing plot of 1

Compound 2. 2 crystallizes in the orthorhombic space group $Pbca$. It consists of 2D azido-bridged Mn^{2+} ions with 3-(pyridinyl)tetrazole anion acting as pentadentate co-ligands. Besides, the 3-(pyridinyl)tetrazole anion acting as the tridentate bridge ligands and pillars the neighboring 2D layers into 3D frameworks. The geometries of them are listed in Table 3.

The structure of 2D azido-bridged Mn^{2+} layer is complicated. There are three crystallographically independent Mn^{2+} ions existent in the symmetrical unit. Each of the Mn^{2+} ions is coordinated octahedrally. $\text{Mn}(1)^{2+}$ is coordinated by six nitrogen atoms, with three azide nitrogen atoms and a tetrazole atom in equatorial

Table 3 Selected bond lengths (nm) and angles ($^\circ$) for 2·Mn

Mn(3)-N(7)	0.220 1(6)	Mn(1)-N(18)	0.224 1(6)	N(10)-Mn(1) ^b	0.217 8(6)
Mn(3)-N(10)	0.221 2(6)	Mn(1)-N(17)	0.225 5(5)	N(16)-Mn(3) ^d	0.229 0(5)
Mn(3)-N(13)	0.223 5(6)	Mn(1)-N(22)	0.229 3(6)	N(3)-Mn(3) ^c	0.223 5(6)
Mn(3)-O(1)	0.223 5(5)	N(15)-Mn(2) ^d	0.226 2(6)	Mn(1)-N(10) ^d	0.217 8(6)
Mn(3)-N(3) ^a	0.223 5(6)	N(6)-Mn(1) ^a	0.211 9(6)	Mn(2)-N(15) ^b	0.226 2(6)
Mn(3)-N(16) ^b	0.229 0(5)	Mn(1)-N(6) ^c	0.211 9(6)	Mn(2)-N(19)	0.227 9(5)
N(7)-Mn(3)-N(3) ^a	91.6(2)	N(22)-Mn(1)-N(1)	5.12(19)	N(6)c-Mn(1)-N(17)	176.5(2)
N(10)-Mn(3)-N(3) ^a	90.4(2)	C(22)-N(15)-Mn(2) ^d	139.6(4)	C(6)-N(13)-Mn(3)	126.2(5)
O(1)-Mn(3)-N(3) ^a	175.9(2)	N(17)-N(16)-Mn(3) ^d	121.1(4)	N(7)-Mn(2)-N(15) ^b	88.0(2)
N(7)-Mn(3)-N(16) ^b	84.4(2)	N(15)-N(16)-Mn(3) ^d	126.0(4)	N(1)-Mn(2)-N(15) ^b	97.2(2)
N(10)-Mn(3)-N(16) ^b	85.3(2)	N(6)c-Mn(1)-N(22)	94.5(2)	O(1)-Mn(3)-N(16) ^b	80.21(18)
N(13)-Mn(3)-N(16) ^b	170.8(2)	N(10)d-Mn(1)-N(22)	89.7(2)	N(3)a-Mn(3)-N(16) ^b	98.1(2)

^a $x-1/2, y, -z+1/2$; ^b $-x+1/2, y-1/2, z$; ^c $x+1/2, y, -z+1/2$; ^d $-x+1/2, y+1/2, z$.

position, and two nitrogen atoms from tetrazole and pyridine in the axial position. The central ion $\text{Mn}(2)^{2+}$ locates in an important position; it is connected with $\text{Mn}(1)^{2+}$ ions through two tetrazoles and an EO azide bridge as labeled Mn1A and Mn1B in Fig.4. Besides, $\text{Mn}(2)^{2+}$ ion is connected with $\text{Mn}(3)$ ion through a tetrazole and an EO azide ion, and is connected with next neighbor-ing $\text{Mn}(3)^{2+}$ ion with EE azide ions as labeled Mn2A and Mn3B. Thus, $\text{Mn}(2)$ is surrounded by three azide ions and three tetrazole rings in the octahedral geometry. The distance between neighboring Mn (2) and Mn (1) is 0.370 2 nm. As shown in Fig.4, $\text{Mn}(3)$ is connected with neighboring $\text{Mn}(1)$ and $\text{Mn}(2)$ through EO azide ions, and is connected with next neighboring $\text{Mn}(1)$ and $\text{Mn}(2)$ ions with μ -1,1,3 azide ion. The geometry is $\text{Mn3} \cdots \text{Mn1} = 0.381\ 2\ \text{nm}$, $\text{Mn3} \cdots \text{Mn2} = 0.380\ 1\ \text{nm}$, the angle $\text{Mn3-N-Mn1} = 120.53^\circ$, $\text{Mn3-N-Mn2} = 119.33^\circ$, which has large values. Besides, $\text{Mn}(3)$ is connected with $\text{Mn}(1)$ and $\text{Mn}(2)$ ions in the neighboring 2D layer through the tridentate bridge ligand with a 3-(pyridinyl)tetrazole which is pillared between layers. The rest coordinating position of $\text{Mn}(3)$

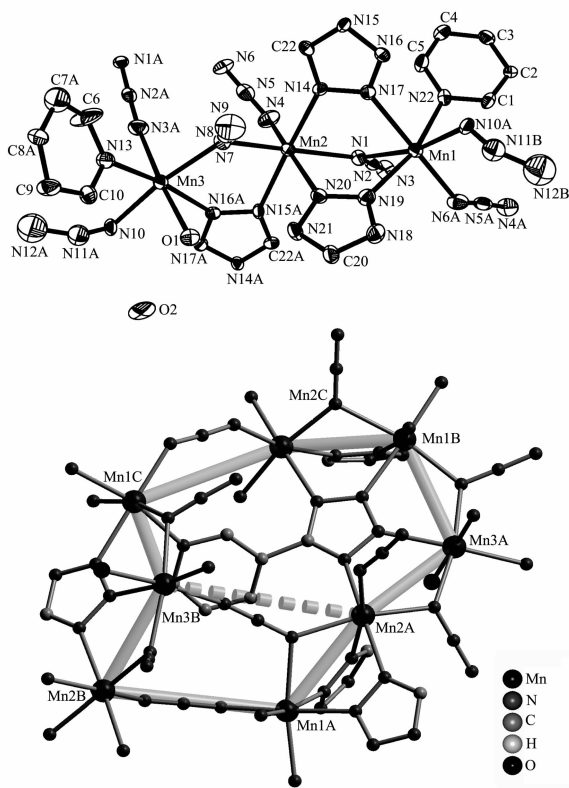


Fig.4 Coordination environment of Mn^{2+} ions and the perspective view of eight member ring of **2**

is occupied by an oxygen atom from water molecule. Thus, the equatorial position of $\text{Mn}(3)$ is occupied by four nitrogen atoms from two azide ions, pyridine and tetrazole rings, and the axial position is occupied by an oxygen atom from water molecule and a nitrogen atom from azide ions. While coordinating to the Mn ions, the 3-(pyridinyl)tetrazole acts as a pentadentate bridge ligand that uses tetrazole ring to connect with four Mn ions around it, and uses 3-pyridine nitrogen to connect with the fifth Mn^{2+} ion. Along with the other three neighboring Mn^{2+} ions connecting through azide ion, they form an eight member ring which are the repeating unit of the 2D layer. The topology of **2** is shown in Fig. 5. The three independent Mn^{2+} ions are arranged in a regular sequence and constructed a (6, 3) topology. The two of separated Mn^{2+} ions are also connected through azide ions, which are labeled Mn3B and Mn2A in Fig.4. It could also be considered that this 2D layer is the tessellation of hexagons and tetragons, as divided by the broken line in Fig.4.

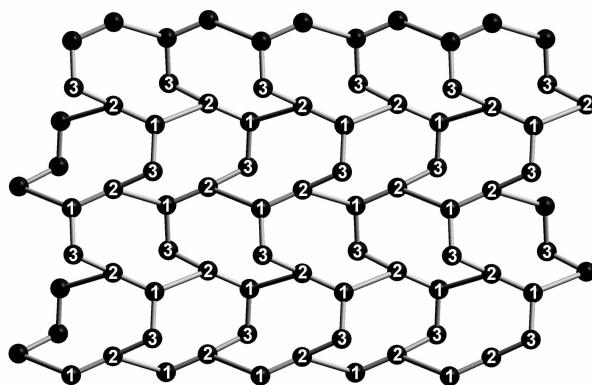


Fig.5 Perspective view of 2D layer of **2**

As is mentioned above, the $\text{Mn}(3)^{2+}$ ions are connected through tridentate 3-(pyridinyl)tetrazole anion with $\text{Mn}(1)$ and $\text{Mn}(2)$ in the neighboring layer. The nearest distance between neighboring layers is $\text{Mn3} \cdots \text{Mn1} = 0.845\ 6\ \text{nm}$. The connection between neighboring layers along *ac* planes are shown in Fig.6. The 3-(pyridinyl)tetrazole anion is sketched in tridentate pillar with the bidentate end representing tetrazole rings and the other end representing pyridine. The dark gray net represents the cross sections of 2D Mn^{2+} layers. One detailed structure of the 3-(pyridinyl)tetrazole ligand has been represented in Fig.6. H-bonds are observed between coor-

minated water molecules and dissociated water molecules.

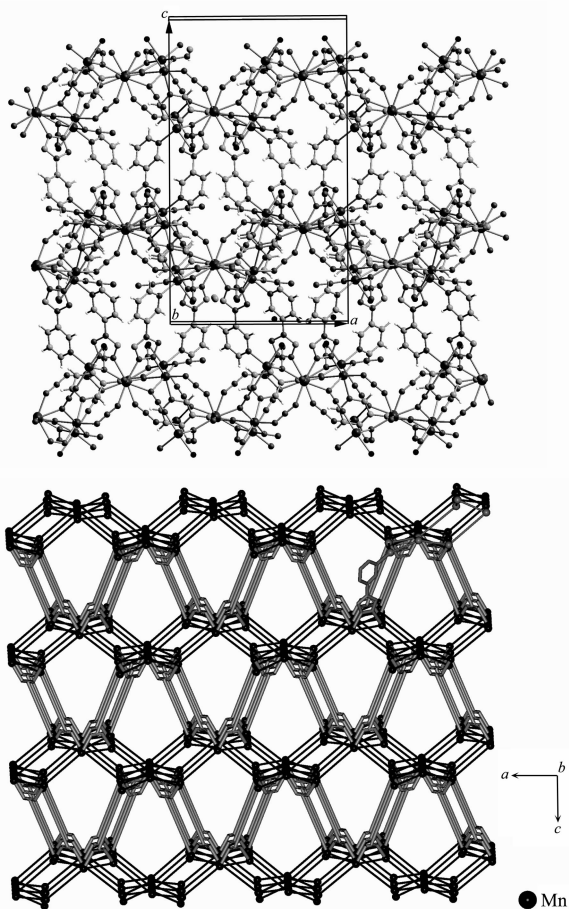
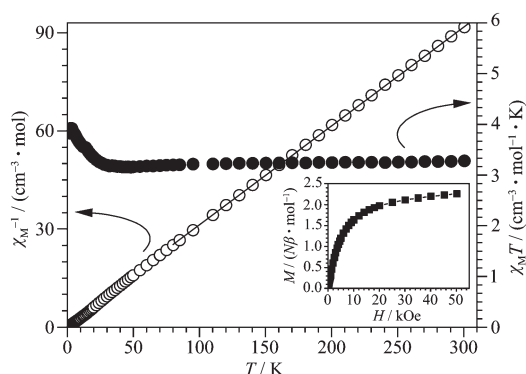


Fig.6 Perspective view of the connection between 2D layers of **2** along the ac plane

2.2 Magnetic properties

Compound 1. The magnetic data of **1** were measured under 1 kOe in the range of 2~300 K, and plotted as χ^{-1} vs T and $\chi_M T$ vs T in Fig.7. The room temperature value of $\chi_M T$ is equal to $3.4 \text{ cm}^3 \cdot \text{mol}^{-1} \cdot \text{K}$, higher than spin-only value for an uncoupled $S=3/2$ ion. The plot of $\chi_M T$ exhibits a slight decrease upon cooling from room temperature, and rise up below 30 K, and reaches an apex around 3 K. The magnetic susceptibility above 100K obeys the Curie-Weiss law ($\chi_M = C/(T-\theta)$), with C of the $3.3 \text{ cm}^3 \cdot \text{mol}^{-1} \cdot \text{K}$ and θ of -3.1 K . The Curie constant is much larger than expected, indicating the orbital contribution of Co^{2+} ions, while the very small and negative θ suggests a very weak coupling or a possible ferromagnetic interaction. The increase of $\chi_M T$ below 30 K confirms the ferromagnetic interaction between Co^{2+} ions.



Inset displays the magnetization of **1** at 2 K

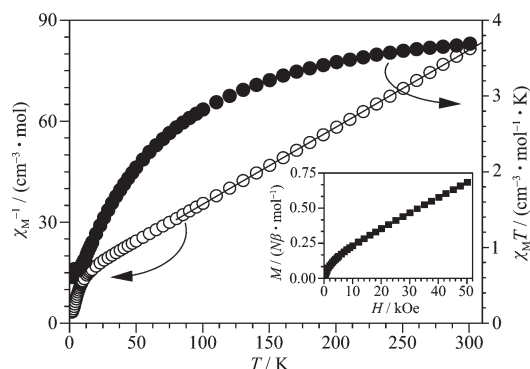
Fig.7 Thermal variation of $\chi_M T$ vs T and χ_M^{-1} vs T for **1**

The field dependent magnetization has been measured at 2 K, as shown in the inner plot. The magnetization increases rapidly for spontaneous along the field and reaches $2.3N\beta$ at 50 kOe, close to the expected saturated value per Co^{2+} unit.

According to the crystal structure of **1**, the magnetic properties should be attributed to the competition between antiferromagnetic coupling transmitted by EE mode azide ions, the nitrogen atoms of tetrazole rings and ferromagnetic coupling transmitted by EO mode azide ion. In the azido-bridged 1D chain of **1**, the EO azide ions connect two neighboring Co ions into dimer along with two tetrazole rings. While EE azide ions connect dimers into 1D chain and form a magnetic structure with AF-FM-AF-FM alternatively. The competition between FM and AF couplings are existed along the chain, and the resulting dominant magnetic coupling is ferromagnetic. Although the 1D azido-bridged Co^{2+} band is connected by the conjugate ligand system and mononuclear Co^{2+} ion, the magnetic coupling hasn't spread along 2D. No long range order has been observed above 2 K. While because of the appearance of the apex on $\chi_M T$ curve, phase transition should appear below it.

Compound 2. As shown in Fig.8, the magnetic susceptibility of **2** has been measured in the range of 2~300 K under 1 kOe. The room temperature value of $\chi_M T$ is equal to $3.7 \text{ cm}^3 \cdot \text{mol}^{-1} \cdot \text{K}$, it exhibits a gradually reduce upon further cooling. The Curie-Weiss fit of data above 50 K give the C of $4.36 \text{ cm}^3 \cdot \text{mol}^{-1} \cdot \text{K}$ per and θ of -54.1 K . The value of C and $\chi_M T$ are comparable to the spin-only value for Mn^{2+} , the big negative value of θ

indicates the strong antiferromagnetic coupling. No long range order of **2** has been observed above 2 K.



Inset displays the magnetization of **2** at 2 K

Fig.8 Thermal variation of $\chi_M T$ vs T and χ_M^{-1} vs T for **2**

The isothermal magnetization of **2** was measured at 2 K (Fig.8). The molar magnetization curve exhibits a quick increase below 1 kOe, and then follows a linear increase till 50 kOe with the effective moment of $0.68N\beta$, which is far from the expected saturation value per unit Mn^{2+} ion with $S=5/2$ owing to the existence of strong antiferromagnetic interaction.

According to the crystal structure, the magnetic couplings between Mn^{2+} ions are transmitted by three routes, EO and EE azide ions and the nitrogen atoms on tetrazole rings. As mentioned in the crystal structure, in the dimers bridged by EO azide, the Mn-N-Mn angle has very large values which are exceeded than the critical value 104° and reach the antiferromagnetic coupling region^[31]. Thus, all the azide ions transmit antiferromagnetic couplings and the tetrazole rings also transmit somewhat antiferromagnetic couplings too. These routes of couplings interpret the strong couplings between Mn^{2+} ions revealed in the measurements.

References:

- [1] Ye Q, Song Y M, Wang G X, et al. *J. Am. Chem. Soc.*, **2006**, **128**:6554~6555
- [2] Ye Q, Li Y H, Song Y M, et al. *Inorg. Chem.*, **2005**, **44**:3618~3625
- [3] Wang X S, Tang Y Z, Huang X F, et al. *Inorg. Chem.*, **2005**, **44**:5278~5285
- [4] Ye Q, Tang Y Z, Wang X S, et al. *Dalton Trans.*, **2005**:1570~1573
- [5] Demko Z P, Sharpless K B. *J. Org. Chem.*, **2001**, **66**:7945~7950
- [6] Demko Z P, Sharpless K B. *Org. Lett.*, **2001**, **3**:4091~4094
- [7] Demko Z P, Sharpless K B. *Org. Lett.*, **2002**, **4**:2525~2527
- [8] Demko Z P, Sharpless K B. *Angew. Chem., Int. Ed. Engl.*, **2002**, **41**:2110~2113
- [9] Himo F, Demko Z P, Noodleman L, et al. *J. Am. Chem. Soc.*, **2003**, **125**:9983~9987
- [10] Gaponik P N, Voitekhovich S V, Lyakhov A S, et al. *Inorg. Chim. Acta*, **2005**, **358**:2549~2557
- [11] Satoh Y, Marcopulos N. *Tetrahedron Lett.*, **1995**, **36**:1759~1762
- [12] Lin P, Clegg W, Harrington R W, et al. *Dalton Trans.*, **2005**:2388~2389
- [13] Wu T, Yi B H, Li D. *Inorg. Chem.*, **2005**, **44**:4130~4132
- [14] Mautner F A, Gspan C, Gatterer K, et al. *Polyhedron*, **2004**, **23**:1217~1224
- [15] Xue X, Wang X S, Wang L Z, et al. *Inorg. Chem.*, **2002**, **41**:6544~6546
- [16] Sen W X, Feng H X, Gen X R. *Chin. J. Inorg. Chem.*, **2005**, **21**:1020~1024
- [17] Wang G X, Bo L, Xiong R G. *Chin. J. Inorg. Chem.*, **2007**, **23**:1997~1998
- [18] Wang L Z, Qu Z R, Zhao H, et al. *Inorg. Chem.*, **2003**, **42**:3969~3971
- [19] Qu Z R, Zhao H, Wang X S, et al. *Inorg. Chem.*, **2003**, **42**:7710~7712
- [20] Abu-Youssef M A M, Mautner F A, Massoud A A A, et al. *Polyhedron*, **2007**, **26**:1531~1540
- [21] Stassen A F, Driessen W L, Haasnoot J G, et al. *Inorg. Chim. Acta*, **2003**, **350**:57~61
- [22] "HKL2000" and "maXus" Softwares, University of Glasgow, Scotland, UK, Nonius BV, Delft, The Netherlands and MacScience Co. Ltd., Yokohama, Japan, **2000**.
- [23] "Collect" Data Collection Software, Nonius B V, Delft, The Netherlands, **1998**.
- [24] Blessing R H. *Acta Crystallogr.*, **1995**, **A51**:33~58
- [25] Blessing R H. *J. Appl. Crystallogr.*, **1997**, **30**:421~426
- [26] Sheldrick G M. *SHELX-97, PC Version*, University of Göttingen, Germany, **1997**.
- [27] Sheldrick G M. *SHELXTL Version 5.1, Bruker Analytical X-ray Instruments Inc.*, Madison, Wisconsin, USA, **1998**.
- [28] Boudreaux E A, Mulay J N. *Theory and Application of Molecular Diamagnetism*. J. Wiley and Sons, New York, **1976**.
- [29] Rodríguez-Diéguez A, Salinas-Castillo A, Galli S, et al. *Dalton Trans.*, **2007**:1821~1828
- [30] Xiong R G, Xue X, Zhao H, et al. *Angew. Chem. Int. Ed.*, **2002**, **41**:3800~3803
- [31] Ruiz E, Cano J, Alvarez S, et al. *J. Am. Chem. Soc.*, **1998**, **120**:11122~11129